

## A Low Cost Ultrasound-based Localisation System for Ground Robotics

**Alec BURNS, Sebastiano FICHERA and \* Paolo PAOLETTI**

School of Engineering, University of Liverpool, Brownlow Hill, Liverpool L69 3GH, UK

Tel.: 44 151 7945232

\* E-mail: P.Paoletti@liverpool.ac.uk

*Received: 30 August 2019 /Accepted: 15 October 2019 /Published: 30 November 2019*

---

**Abstract:** This paper presents a low-cost localisation system based on ultrasonic sensing and time of flight measurements. A compact ultrasound emitter has been designed to generate an omnidirectional train of ultrasound pulses which are then picked up by several fixed receivers measuring the time difference of arrival. A least squares approach is used to analytically obtain a first estimate of the emitter position, which is then refined through steepest descent optimisation. All processing is done via a standard Arduino platform, proving the low computational demands of the method. Localisation results are validated against a state-of-the-art Optitrack motion capture system. It is shown that the system can cover a  $4.3 \times 3.1$  m arena with a mean error localisation error of 1.57 cm and an average standard deviation of 1.39 cm throughout the arena. The effectiveness of the proposed localization system is demonstrated by integrating it with a mobile ground robot to enable waypoint-based path following.

**Keywords:** Localisation, Ultrasound, Time difference of arrival, Positioning, Ground robots.

---

### 1. Introduction

Ground robots are becoming increasingly popular platforms for research, industry and hobbyists alike. As the rise in demand has continued, so too has the need for these devices to be compact, simple and inexpensive, yet accurate and robust. The ability to determine their position within the surrounding environment is a critical enabling capability in order for a mobile robot to move around and interact with large scale environments [1].

Over the years, several methods have been developed to tackle the localization challenge. For lower-end robots, i.e. simple low-cost robots with limited computational power, dead-reckoning methods have been widely used. This method is based on local sensors feedback, e.g. encoder readings in wheeled robots. Knowledge of the starting position

and distance travelled allows one to estimate current position. However, small inaccuracies and drifts in the system, such as slippage of the wheels, may lead to large errors over long distances if not properly compensated for [2].

Another popular option is Visual Positioning Systems (VPS) that compare the current scene with previously stored scenes to create a best estimation of current location. Recent developments in the field have made this technique a viable option for localisation [3]. However, the relatively high computational cost and hardware complexity make this approach not suitable for implementing a real-time low-cost localisation system [4]. Also, VPS require a prior knowledge of the map within which they will operate, preventing them to be used in unknown, dynamic or unstructured environments.

Localisation solutions based on external sensory networks may provide an effective solution for satisfying accuracy requirements while meeting low-cost constraints. One such solution is the Active Bat system, a broadband ultrasonic position system utilizing Time-of-Flight information from the badges to a network of receivers on the ceiling and calculates the 3D positions of the badges using a multilateration algorithm. This system achieves a 2D accuracy of approximately 2 cm. However, the coverage of 1000 m<sup>2</sup> is attained with 750 receivers required [5].

Another example is Lok8, an indoor posing system for smartphones that uses off-the-shelf smartphone speakers to produce ultrasound signals (operating at around 22 kHz). The systems accuracy was tested in a 49 m<sup>2</sup> with 4 receivers and achieved an accuracy of around 10cm on average [6].

Commercially available systems can achieve precision up to  $\pm 2$  cm while costing less than £500, see [7] for an example which relies on a series of stationary ultrasonic receiver modules and one mobile emitter module. The location of the mobile emitter module is calculated based on propagation delay of the signal. Another commercially available localisation solution, which utilizes a similar positioning algorithm is described in [8]. This product relies on Ultra-Wide Band (UWB) wave propagation instead of ultrasonic signals, is available for just under \$1000 and is a centimetre-level accurate positioning system.

In this work, a novel low-cost localisation system based on ultrasound sensing is described and validated against a state-of-the-art motion tracking system. It is shown that such localisation platform is able to provide good accuracy while requiring very limited sensing and computational complexity.

This paper is organised as follows. Section 2 motivates the design choices for the localisation system, which is then presented in detail in Section 3. Section 4 describes the hardware setup used to assess the quality of the proposed solution, and results from such assessment are discussed in Section 5. Finally, some conclusions are drawn in Section 6, together with suggestions for future research directions.

## 2. Definition of the Infrastructure

Various factors need to be taken in consideration when designing or assessing any localisation technique, including: accuracy, precision, robustness, financial cost and system simplicity (refer to [9] and [10] for definitions of these metrics).

Wireless indoor localisation approaches can be classified according to two main criteria [9-10].

- Physical sensor infrastructure, i.e. the platform used to detect/sense position;
- Positioning algorithm, i.e. the method to estimate location from sensory data.

The combination of these elements determines the overall method for localising the mobile robots.

## 2.1. Sensor Topology

Most physical sensory infrastructures rely on two aspects: a signal emitter and a measuring unit called a receiver. Measurement involves the transmission and reception of signals between these parts of the system. There are four different system topologies for positioning systems [9]. The Remote Positioning System (RPS) places the emitter unit on the mobile robot at an unknown location. The emitter generates a signal which is received by receivers placed at known fixed locations. The results from the measuring units are collected and the location of the emission source calculated on an external master station. The second topology is Self-Positioning System (SPS) and involves a mobile unit which receives signals of several transmitters placed at known locations and has the capability to compute its location based on the measured signals. Sending the final measurement results from the mobile unit to the remote unit in an SPS is referred to as indirect self-positioning system (ISPS), which is the third type of topology. Finally, transmitting the final measurement result from the remote unit to the mobile unit in an RPS is referred to as Indirect Remote Positioning System (IRPS).

IRPS was selected here as it reduces the need for a mobile robot to have high computational capabilities on board and offsets this function to a ground station. This widens the range of systems the localisation platform could be applied to, especially when considering simple low-level robots, robots with small payload or swarm systems. Furthermore, transmitting the final results from the remote unit to the mobile unit allows all decision making to be done on the mobile robot and, potentially, enables sensor fusion with odometry.

## 2.2. Sensor Types

Within the IRPS family of localisation systems, different choices of signals propagated between the emitter and receivers can be made. Table 1 provides a comparison of the most popular methods available.

The typical dimension of low-cost mobile ground robots is of the order of tens of centimetres, therefore it is reasonable to assume that the localisation system needs to have an accuracy of less than 5 cm. As can be seen from Table 1, this requirement rules out solutions such as RFID, ZigBee and WiFi. UWB could be an option for future development as it is undergoing fast development in terms of accuracy, has strong anti-interference capability and is capable of permeating through objects [12]. However, state of the art UWB-based systems are still not accurate enough to meet the requirement outlined above. For example, in [13] authors achieved accuracies <31 cm in 90 % of position estimates with an average inter-sample noise of 9 cm.

Ultrasound (US) localisation was therefore selected as the most appropriate sensor type due to its

potential high accuracy. Furthermore, due to the slow propagation speed of US waves (340 m/s), simple processing technology can be used, reducing overall complexity. The only drawback of current systems are overall cost and scalability [4, 14]. The system proposed here overcomes these issues, maintaining high accuracy on a large arena while being

significantly less expensive than commercially available platforms.

The use of the ultrasonic platform within an IRPS topology is novel due to the difficulties presented in designing a central ‘omnidirectional’ ultrasonic emitter, the details of which are presented in Section 4.1.

**Table 1.** Comparison of main indoor positioning technologies [4, 10].

System	Accuracy	Coverage	Methods	Topology	Scale	Complexity	Cost
IR	57 cm-2.3 m	Room	Cell-ID, RSSI, TOA	(I)SPS, (I)RPS	Low	High	High
UWB	15 cm	Building	RSSI, TOA, TDOA, AoA	(I)RPS	Low	Low	High
US	1 cm-2 m	Room	ToA, TDoA	(I)RPS	Low	Low	High
WiFi	1.5 m	Building	Cell-ID, RSSI, TOA, AoA	(I)SPS, (I)RPS	High	Low	Low
BT	30 cm-meters	Building	Cell-ID, RSSI, TOA	(I)SPS	High	Low	High
RFID	1-5 m	Room	Cell-ID, RSSI	(I)SPS,(I)RPS	Medium	Low	Low
ZigBee	30 cm-meters	Building	Cell-ID, RSSI	(I)SPS, (I)RPS	Low	Low	Medium
Audible Sound	Meters	Room	ToA, TDoA	(I)RPS	Low	Low	High
GPS	6 m-10 m	Global	ToA	(I)SPS	Low	High	High

### 3. Localisation Estimation Algorithm

The proposed system consists of a central ‘omnidirectional’ point emitter to be localised and a series of fixed directional receivers at known locations.

Time-Difference-of-Arrival (TDoA) was selected as the approach to estimate emitter position. When compared with other approaches such as Angle-of-Arrival or Time-of-Arrival, TDoA systems are cheaper and simpler in both hardware and computational algorithm [4, 15, 16]. For TDoA, an omnidirectional US signal is generated from the mobile emitter. As this pulse reaches the first receiver, the time of reception  $t_0$  is recorded. Furthermore, as the US pulse continues to travel, it will continue triggering receivers which will also record times *relative* to the first receiver  $t_{i0} = t_i - t_0$ . These relative times of reception allow localization of the emitter on a hyperboloid with the first receiver and  $i$ -th receiver positions as foci [17]. Mathematically, this translates into the system of equations [18].

$$\begin{aligned}
 (x - x_0)^2 + (y - y_0)^2 + (z - z_0)^2 &= (t_0 + t_{00})^2 v_s^2 \\
 (x - x_1)^2 + (y - y_1)^2 + (z - z_1)^2 &= (t_0 + t_{10})^2 v_s^2, \\
 &\vdots \\
 (x - x_N)^2 + (y - y_N)^2 + (z - z_N)^2 &= (t_0 + t_{N0})^2 v_s^2
 \end{aligned} \tag{1}$$

where  $v_s$  is the speed of the US signal,  $(x, y, z)$  are the unknown emitter coordinates and  $(x_i, y_i, z_i)$  is the known positions of the  $i$ -th receiver. Note that  $t_{00} = 0$  by definition.

#### 3.1. Initial Localisation via Triangulation

The physical infrastructure described in Section 2 and the TDoA approach described in Section 3 provides a series of hyperboloids theoretically intersecting at the emitter location. However, noise in signal propagation, received signal measurement and location of receivers translates to an uncertainty in the estimation of emitter position. Closed-form solutions for the localisation problem do not accommodate for situations where hyperboloids do not intersect at a single point [19], therefore best approximations algorithms are always necessary. An analytical solution to best-fit the emitter position in TDoA systems has been proposed in [18] and is used as a first step in the algorithm proposed in this paper.

To this end, the first line of Eq. (1) is subtracted from the subsequent lines, thus obtaining

$$2A\mathbf{p} = \mathbf{b}, \tag{2}$$

where

$$A = \begin{bmatrix} x'_1 & y'_1 & z'_1 & t_{10} v_s^2 \\ x'_2 & y'_2 & z'_2 & t_{20} v_s^2 \\ \vdots & \vdots & \vdots & \vdots \\ x'_N & y'_N & z'_N & t_{N0} v_s^2 \end{bmatrix}, \mathbf{p} = \begin{bmatrix} x \\ y \\ z \\ t_0 \end{bmatrix} \tag{3}$$

$$\mathbf{b} = \begin{bmatrix} x_1^2 - x_0^2 + y_1^2 - y_0^2 + z_1^2 - z_0^2 - t_{10} v_s^2 \\ x_2^2 - x_0^2 + y_2^2 - y_0^2 + z_2^2 - z_0^2 - t_{20} v_s^2 \\ \vdots \\ x_N^2 - x_0^2 + y_N^2 - y_0^2 + z_N^2 - z_0^2 - t_{N0} v_s^2 \end{bmatrix}$$

and  $x'_i = x_i - x_0, y'_i = y_i - y_0, z'_i = z_i - z_0, i = 1, \dots, N$ .

The solution of this system of linear equations then provides the emitter position  $\mathbf{p}$ . As mentioned before, presence of noise and uncertainties implies that no exact solution exists, therefore a Least Squares algorithm was used here to solve Eq. (1) with minimal computational cost [20]

$$\mathbf{p} = \left(\frac{1}{2}\right) (A^T A)^{-1} A^T (\mathbf{b}) \quad (4)$$

Note that this solution is simpler than the one described in [18] as it provides  $\mathbf{p}$  in a single step and does not involve second order equations which may lead to multiple solutions. However, as matrix inversion ( $A^T A$ ) is required, the matrix  $A^T A$  must be non-singular. According to the definition of the matrix  $A$  in Eq. (3), singular configurations may occur if, for example, all the receivers lay on the same plane (in this case one of the first three columns is zero), or if more than  $N-4$  receivers are in the same point (in this case  $N-4$  rows are linearly dependent). These pathological situations can be easily avoided by placing the receivers accordingly. Lastly, errors will occur if all values of the fourth column of matrix  $A$  are *exactly* the same, that is if all receivers are the exact same distance away from the closest receiver to the robot. Once again, this situation is unlikely to occur in practice if the receivers are positioned correctly. Therefore Eq. (4) provides a robust and fast method to obtain a first estimate of the emitter location.

The solution proposed here, unlike the one described in [18], is based on a system that relies on one emitter and multiple receivers, with the algorithm being shaped on this assumption. The use of a single central emission pulse per cycle avoids the need for time scheduling between different transmitters. On the other hand, the system described in [18] requires a 65ms time allocation per emitter, reducing overall scalability. Moreover, the solution proposed here removes the requirement for the ultrasonic transmitters to emit signals with known periods and order, thus further reducing system complexity.

### 3.2. Localisation Improvement Via Optimization

There are several sources of noise and uncertainty in the system, therefore an optimisation procedure is used to minimise the effect on such factors on localisation accuracy. The algorithm described in Section 3.1 provides a good first estimate of the emitter location, but its accuracy is limited by the presence of noise and uncertainty limits. Therefore, the estimate obtained in Eq. (4) is used as first guess in an iterative optimization procedure aimed at improving localisation accuracy by adjusting the estimate  $\mathbf{p}$ . Such optimization problem can be mathematically expressed as

$$\mathbf{p}_{estimated} = \underset{\mathbf{p}_0}{\operatorname{argmin}} [S(\mathbf{p})] \quad (5)$$

$$S(\mathbf{p}) = \sum_{i=1}^N [(x - x_i)^2 + (y - y_i)^2 + (z - z_i)^2 - (t_0 + t_{i0})^2 v_{sound}^2]^2 \quad (6)$$

A simple steepest descent algorithm is proposed to solve such problem. Note that Gauss-Newton or Levenberg-Marquardt are often preferred thanks to their superior convergence properties [21], but they require significantly more computational and memory resources. Moreover, simulation results indicate that such more advanced methods do not offer significant improvement compared to the simpler steepest descent method for the localisation scenario considered here.

The pseudo-code of the implemented steepest descent algorithm proposed for the localisation platform is shown in Table 2. Both the step size and the stopping criterion for these experiments were chosen heuristically. The step size was optimized to ensure convergence without requiring too many steps and the stopping criterion ensures that as soon as convergence occurs, the iterative minimiser stops. The constraint  $k < k_{max}$  is included to terminate the iterative process so that there exists an upper bound for its execution time. In fact, very often (e.g. for real mobile robotic control) it is more important to get position estimates with a good rate, even at the expenses of accuracy. Moreover, it is worth noting that most of the benefits of steepest descent are realised in the first few iterations [23], therefore even a small value of  $k_{max}$  is sufficient to significantly improve accuracy with respect to the estimate provided by Eq. (4).

**Table 2.** Pseudo-code for solving problem Eqs. (5)-(6).

<ol style="list-style-type: none"> <li>1. Initialise <math>\mathbf{p}_{estimated}(\mathbf{1})</math> with results from Eq. (4)</li> <li>2. Calculate step direction <math>\mathbf{step}(k) = -\nabla S(\mathbf{p}_{estimated}(k))</math></li> <li>3. Perform an optimisation step, with a predetermined step size <math>\alpha</math> <math>\mathbf{p}_{estimated}(k+1) = \alpha \cdot \mathbf{step}(k) + \mathbf{p}_{estimated}(k)</math></li> <li>4. Check the stopping criterion for convergence</li> <li>5. If the stopping criterion is not satisfied and <math>k &lt; k_{max}</math> repeat steps 2-5, otherwise return <math>\mathbf{p}_{estimated}(k)</math></li> </ol>
-----------------------------------------------------------------------------------------------------------------------------------------------------------------------------------------------------------------------------------------------------------------------------------------------------------------------------------------------------------------------------------------------------------------------------------------------------------------------------------------------------------------------------------------------------------------------------------------------------------------------------------------------------------------------------------------

For the results shown in this paper we used  $k_{max} = 40$  and the stopping criterion  $|\mathbf{p}_{estimated}(k) - \mathbf{p}_{estimated}(k-1)| < 0.0002$ . On the standard Arduino Mega 2560 platforms used for validation it takes on average 0.7 s to get the final estimate for emitter location, of which about 0.3 s are spent for running the minimisation algorithm.

## 4. Experimental Setup for Validation

To validate the performance of the proposed localisation system have been validated by

implementing it and comparing its accuracy against a state-of-the-art motion tracking system, as described in this section.

#### 4.1. Validation Setup

The processor unit utilised is an Arduino Mega 2560, which detects signals from the receivers and runs algorithm 1 and 2 for localisation. The output of this Arduino is connected to a Raspberry Pi to transmit all coordinates to a laptop to make a comparison with the coordinates provided by a motion tracking system composed of 8 Optitrack Prime 17W cameras. The emitter unit also utilizes an Arduino Mega 2560 board to trigger emission. Both units are connected via an RF transmitter/receiver (ERA-ARDUINO-S900) to trigger a new emission only once the localisation algorithm is finished. Motion capture results are captured at 100 Hz, whereas algorithm 2 takes about 0.7 s to run on the Arduino Mega 2560 board. To synchronise these two datasets, motion capture results are acquired and stored until the localiser has calculated a position, and then the nearest pair of coordinates from the 10 most recently acquired points is chosen to perform the comparison. Note that the robot used for moving the emitter has a speed of less than 1 cm/s, therefore such synchronisation strategy is accurate.

#### 4.2. Description of the Hardware Implementation

The 12 receivers used are composed of US ceramic transducers (MCUSD16A40S12RO), which resonate at 40 kHz when detecting the pulse generated by the emitter. The received signal is then amplified 8-fold by a three-stage analogue amplifier and then converted to a square wave via a Schmidt-comparator (LM386). This signal processing electronics was inspired by the one described in [22]. The threshold value of the Schmidt-comparator was chosen to maximise range while avoiding the possibility of signal noise being amplified. For the setup described in this paper values between  $\sim 0.04$  V and  $\sim 0.9$  V provided a good trade-off between range and noise removal. This output of the Schmidt-comparator is then rectified and filtered by a passive Low Pass Filter at 15.9 kHz. Finally, a comparator (LM339-N) with cut off voltage is 1.9 V is used to generate the trigger signal to be transmitted to the processing unit.

The emitter is composed by 13 US transducers (MCUSD16A40S12RO), with their outer metallic case removed to reduce the directionality properties. The support for such transducer was designed and 3D-printed so that an (almost) omnidirectional emission was achieved, as shown in Fig. 1. By doing this, the emitter can be considered a point source as required by the localisation algorithm described in Section 3. The 13 transducers are simultaneously pulsed using a

microcontroller (PIC12F1822) generating a 40 kHz square wave, which is then amplified via a MOSFET amplifier and fed to the US emitters.

Experimental tests highlighted that the number of pulses affects the performance of the localisation system both in terms of coverage and accuracy. More pulses result in increased coverage but decreased accuracy, and vice versa. As reported in Fig. 2, the mean overall error across the arena is proportional to the number of pulses. When a single pulse is emitted, the initial time  $t_0$  will be identical for any active receiver. However, if there are two pulses and some receivers pick up the first pulse and some receivers pick up the second pulse, then  $t_{i0}$  may be different for these two sets of receivers, thus introducing additional uncertainty and increasing the localisation error. This effect may become significant for larger numbers of pulses. In fact, at 40 kHz, the time between pulses is  $12.5 \mu\text{s}$ , which corresponds to 4.3 mm/pulse with a speed of sound  $v_{\text{sound}} = 343 \text{ m/s}$ . However, this uncertainty is significantly mitigated by the optimiser. On the other hand, the coverage of the system relies solely on the number of receivers picking up a signal at any given emission. Given the receiver circuits used, a weak reception may not always be immediately detected from the first pulse and could take multiple pulses from the same signal before detection is triggered. Therefore, the more pulses being transmitted, the more likely a receiver will register a reception and the higher the coverage is, as shown in Fig. 3. The optimal number of pulses for the setup used for validation was determined to be five to ensure almost complete coverage while retaining good accuracy.



Fig. 1. 'Omnidirectional' US transducer array for the emitter.

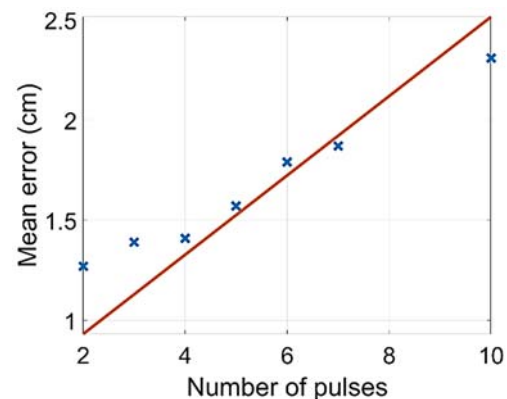


Fig. 2. Mean error (cm) vs. number of pulses.

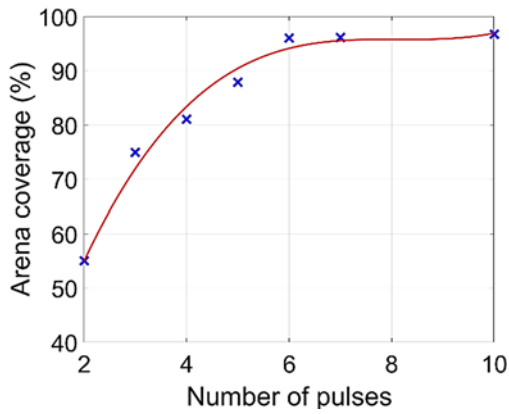


Fig. 3. Arena coverage (%) vs. number of pulses.

## 5. Results

Testing was done in a motion capture arena of approximately 4.3 m by 3.1 m, the emitter unit was placed on board a Create 2 Programmable Robot (iRobot, USA), that performed random movement around the arena for up to 1 hour per test. The results from both the localiser and motion capture were stored offline during this time. The system was tested at four different emitter heights from the floor: 280 mm, 355 mm, 457 mm and 592 mm, to prove its robustness. A summary of the results obtained of these experiments is reported in Table 3.

The 'pre-minimiser results' are obtained using Eq. (4), whereas results from the optimization routine described in Section 3 are referred as 'post-minimiser results'. Finally, given that the robot cannot move faster than approximately 1 cm/s and that algorithm 2 provide results every 0.7 seconds, any localisation estimate that is more than 15 cm apart from the last estimate can be considered as outlier and removed. Such outlier removal provides the set of 'post-filter results'. As can be seen in Table 3, localisation performance has similar trends across all the tested heights. In the following, only the results attained at 355 mm altitude are reported as illustrative examples.

Table 3. Localisation results at different heights.

Height (mm)	Mean Error Post-Filt (cm)	Points with error <1 cm Post-Filt (%)	Points with error <3cm Post-Filt (%)	Coverage (%)
280	1.61	40.1	87.9	87.87
355	1.57	43.05	88.69	93.40
457	1.81	36.43	85.45	86.27
592	1.62	41.06	89.08	79.40

### 5.1. Pre-Minimiser

The pre-minimiser results obtained by Eq. (4) and shown in Fig. 4 are quite inaccurate. In fact, only 14.2 % of the results are within 1 cm of the true

position, 47.8 % are within 3 cm and 81.5 % are within 10 cm. The mean error across all attained values is 11.2 cm. Such relatively high mean localisation error is significantly affected by the presence of extremely large errors (>30 cm) due to emitter reflections being picked up on the receiver units, a phenomenon that will be further discussed later.

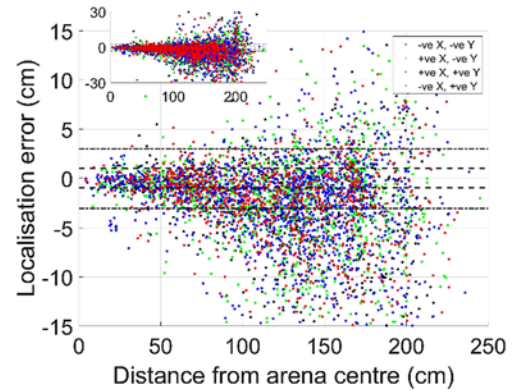


Fig. 4. Pre-Minimiser localisation error (cm) vs distance from arena centre, where different colours are used for the four quadrants of the arena. Inset plot shows a zoomed-out view of the localisation error (range  $\pm 30$  cm).

Another noticeable trend is the monotonic increase of error spread as a function of distance from the centre of the arena. This is likely due to the number of receivers being involved in a positional calculation; as the robot moves away from the centre, some receivers go out of range and therefore less information is provided to the localisation algorithm.

Note that there exist spurious error clusters in certain quadrants, as highlighted in Fig. 5. Upon further inspection, these outliers were the results of some receivers picking up a reflected emission rather than the actual emission. In certain areas, this will happen in such a way that both algorithms will converge on an incorrect location. This could be mitigated by increasing delays between emission, logic filtering or reducing emission strength to decrease reflection likelihood.

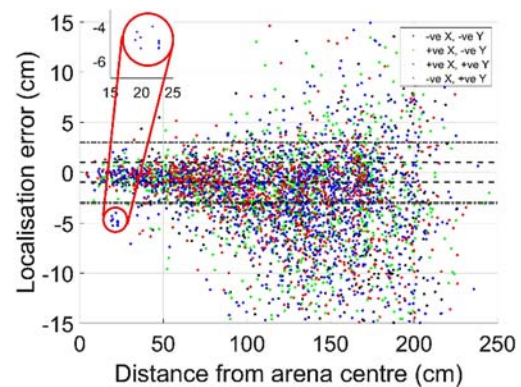


Fig. 5. Highlighted area of reflected reception.



To better quantify accuracy, the heat map shown in Fig. 6 was produced by discretizing the arena on a grid whose cells are 40 cm wide and reporting the median localisation error value for each cell. An ‘Inf’ value within a cell represents an area that has not been explored by the mobile robot during tests, and it is not taken into account when calculating means. The colour scaling is based on how accurate the data is.



Fig. 6. Pre-Minimiser heatmap of the median localisation error (in cm) across the arena. Each cell represents a 40 cm×40 cm region in the arena,

### 5.2. Post Minimiser

After processing the results through the algorithm reported in Table 2, 41.7 % of the results are within 1cm of the true position, almost 3 times as many as the pre-minimised results. Moreover, 85.9 % of results are now within 3 cm and 96.4 % are within 10 cm of true position. Such improved performance translates to an average mean error of 3.33 cm. As shown in Fig. 7, the post minimiser results are more accurate throughout the arena, and the error does not significantly increase as the emitter moves away from the centre of the arena.

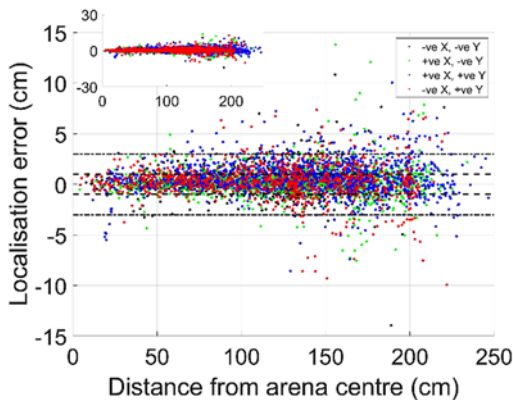


Fig. 7. Post-Minimiser localisation error (cm) vs distance from arena centre where different colours are used for the four quadrants of the arena. Inset plot shows a zoomed-out view of the localisation error (range ±30 cm).

The heat map shown in Fig. 8 demonstrates that the vast majority of results lie well within acceptable tolerances, with only 5 out of 120 cells having median errors above 5 cm.

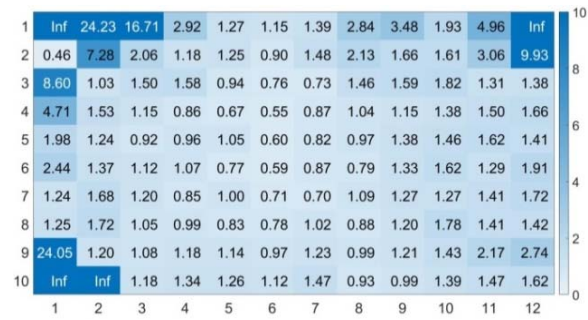


Fig. 8. Post-Minimiser heatmap of the arena, showing median localisation error (in cm) for 40 cm×40 cm cells.

### 5.3. Post Filter

When applying the final filter to remove any value that differs more than 15 cm from the previous estimate, the accuracy improves even further: 43.1 % of the results are within 1 cm of the true position, 88.7 % are within 3 cm and 99.5 % are within 10 cm. The overall average mean error drops to 1.57 cm as well. Fig. 9 reports the heat map related to these results.



Fig. 9. Post-Filter heatmap of the arena, showing median localisation error (in cm) for 40 cm×40 cm cells.

Fig. 10 reports the median error (blue dots and lines) and the mean error (red dots and line) as functions of distance from the arena centre.

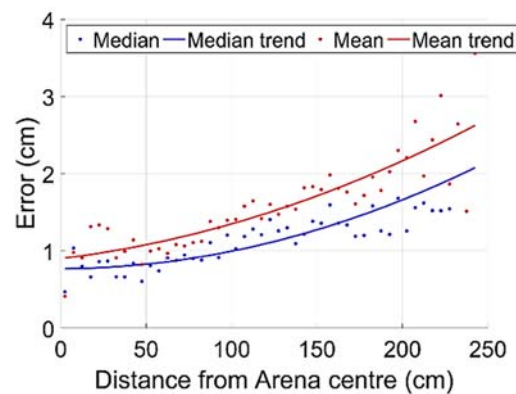
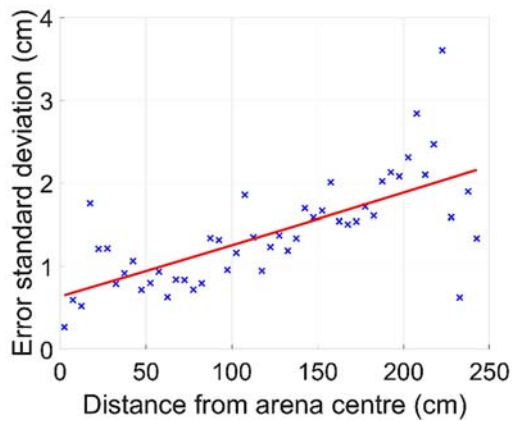


Fig. 10. Median error (red) and mean error (blue) vs distance from arena centre.

Both trends can be fitted by quadratic polynomials with the mean error showing some anomalies at 20 cm from arena centre, which result from the clustered reflections described earlier. The median result is far more robust to such reflection areas and shows a consistently lower error throughout the arena, indicating that the error distribution is skewed. The standard deviation of the results also increases with distance from arena centre as shown in Fig. 11, with an average standard deviation throughout the arena of 1.39 cm.



**Fig. 11.** Standard deviation of localisation errors vs distance from arena centre.

#### 5.4. Localisation Summary

Table 4 summarises the results of each stage of processing, highlighting that the proposed minimisation and filtering algorithms significantly improve localisation performance.

**Table 4.** Summary of results obtained at various processing stages. E=Error, Min=Minimiser, Filt=Filter.

	Mean E	E<1 cm	E<3 cm	E<10 cm
<b>Pre-Min</b>	11.2 cm	14.2 %	47.8 %	81.5 %
<b>Pre-Filt</b>	3.33 cm	41.7 %	85.9 %	96.4 %
<b>Post</b>	1.57 cm	43.1 %	88.7 %	99.5 %

As previously mentioned, reflections played a major role in certain areas and significantly affected mean accuracy in these areas. One way in which this could be mitigated would be the addition of a constant time delay to ensure the dissipation of any remnant signals from previous pulses. Another, much more challenging solution would be the substitution of the Ultrasonic platform to UWB, removing any possible reflections. Usage in open outdoor areas would also remove any reflective areas. Another aspect to consider is the maximum scalability of the system. The current ultrasonic emitters have been tested to ranges of up to 12 m; however, the entire localisation systems accuracy has not been validated beyond the current setup.

#### 5.5. Mobile Ground Robot Integration

To showcase the effectiveness of the proposed localisation platform, a path following demo for ground robots has been developed. To this end, the localisation unit was attached to a tracked robotic platform, as shown in Fig. 12. The integrated mobile robot was then given a series of waypoints that it was required to obtain in sequence to travel along a desired path.

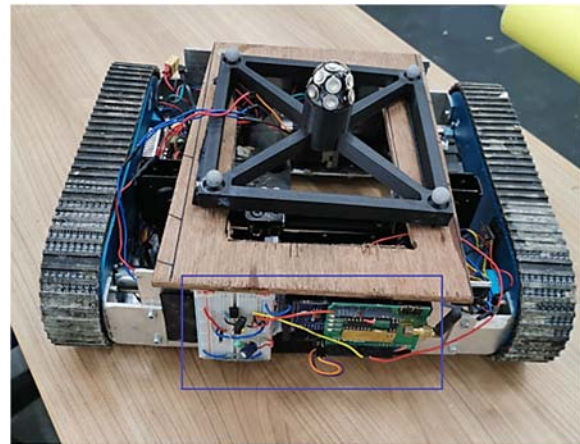


**Fig. 12.** Image of tracked robot integrated with localisation system. The blue box highlights the localisation unit, whereas the omnidirectional emitter surrounded by motion tracking markers was fitted to the top.

The proposed localisation system worked as an independent module that continually acquired positional information at the maximum localisation rate. The master controller of the robot would routinely request the most current (X, Y) coordinates from the localisation unit, which it would then utilise to determine the course of action. Orientation information was acquired using an inertial measurement unit board (Arduino A000070). Provided the most recent position and orientation, the system corrected orientation on the spot to intersect the rover path with the next way point before initiating translational movement in a straight line. Whilst moving towards this waypoint, the system continually performed regular heading checks based on the position and orientation data being acquired periodically. By using this method, the system would reach the waypoint and then proceed to the next waypoint using the same procedure.

It was unrealistic to assume exact heading and waypoint acquisition, therefore tolerances were imposed. Tolerances in heading were variable depending on distance to waypoint, ranging from 3° when the system was over 500 mm from the waypoint, to 15° when the system was less than 70 mm from the waypoint. Waypoint tolerance was set to a constant 25 mm. These values were tuned to ensure the optimum balance between accurate path following and smoothness of movement.



For the purpose of the demo, the system was tasked with following a set of waypoints representing a square whose sides were 170 cm long. Snapshots of the rover achieving the corners of this planned path are shown in Fig. 13.

The rover was also fitted with an array of motion capture markers, as shown in Fig. 12, which enabled more accurate rover path acquisition, using the same technique described in Section 4.1. The results from this test are shown in Fig. 14. The plot consists of over 33,000 motion capture data points acquired over the course of 10 minutes of path following. The red circles shown have a radius of 25 mm and represent the waypoints with the associated tolerance. As can be seen from the results, the waypoints were successfully reached within the specified tolerance. The successful completion of this demo demonstrates that the low-cost ultrasound-based localisation system proposed in this paper is suitable for robotic applications such as path following.



**Fig. 13.** Aerial snapshots of the mobile robot following the predetermined waypoints.

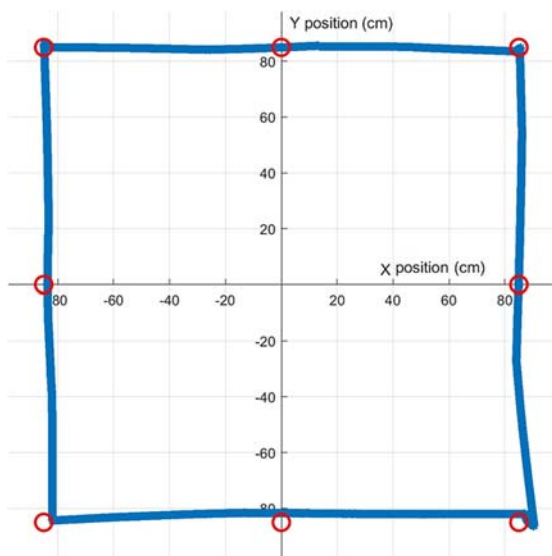


**Fig. 14.** Plot of the mobile unit's exact position shown by the blue line, where the waypoints are highlighted as the centre point with a circle of radius equal to goal tolerance.

## 6. Conclusions

In this paper an inexpensive yet accurate ultrasound-based localisation system is proposed. The total cost of the components is around £100, the biggest share of which are two Arduino Mega 2560 boards used for trigger emission and for processing data at the receivers end. The system allows localisation of 89 % of the 4.3 m × 3.1 m arena with an accuracy of less than 3 cm and 43 % with an accuracy of less than 1 cm. The system has been proven to be scalable between 280 mm and 592 mm of height, without requiring any change in the experimental setup. The proposed localisation system is generic and can be used for a variety of applications [24]. For example, it was integrated with a ground robot to show that it can be successfully used to enable the robot to perform waypoint-based path following.

Given the range of the ultrasound transceivers used, the system should theoretically perform well in arenas up to 12×12×12 m in size. Optimisation of receiver location and orientation and use of more powerful transducers would also allow better performance in larger arenas if needed. Finally, more advanced filtering approaches may be developed to improve robustness with respect to spurious reflections.

## Acknowledgements

This research was supported by Apadana Management 3 Ltd. The authors also wish to thank colleagues from the University of Liverpool who provided insight and expertise that greatly assisted the research.

## References

- [1]. H. Cheng, H. Chen, Y. Liu, Topological Indoor Localization and Navigation for Autonomous Mobile Robot, *IEEE Transactions on Automation Science and Engineering*, Vol. 12, Issue 2, 2014, pp. 729-738.
- [2]. C. C. Ward, K. Iagnemma, A Dynamic-Model-Based Wheel Slip Detector, *IEEE Transactions on Robotics*, Vol. 24, Issue 4, 2008, pp. 821-832.
- [3]. L. Paya, A. Gil, O. Reinoso, A State-of-the-Art Review on Mapping and Localization of Mobile Robots Using Omnidirectional Vision Sensors, *Journal of Sensors*, Vol. 2017, 2017, pp. 1-20.
- [4]. A. A. Khudhair, S. Q. Jabbar, M. Q. Sulttan, D. Wang, Wireless Indoor Localization Systems and Techniques: Survey and Comparative Study, *Indonesian Journal of Electrical Engineering and Computer Science*, Vol. 3, Issue 2, 2016, pp. 392-409.
- [5]. AT&T Laboratories Cambridge, The Bat Ultrasonic Location System, AT&T, 2002. [Online]. Available: <https://www.cl.cam.ac.uk/research/dtg/attarchive/bat/>. [Accessed 23 August 2018].
- [6]. L. Batistic, M. Tomic, Overview of Indoor Positioning System Technologies, *International Convention on Information and Communication Technology*,

- Electronics and Microelectronics (MIPRO)*, Issue 41, 2018, pp. 473-478.
- [7]. Marvelmind Robotics, Starter Set – HW v4.9, August 2018. [Online]. <https://marvelmind.com/product/starter-set-hw-v4-9-plastic-housing/>. [Accessed August 2018].
- [8]. Seeed, UWB PK-1000 Standard Edition, Pudutech, 2017. [Online]. <https://www.seeedstudio.com/UWB-PK-1000-Standard-Edition-p-2918.html>. [Accessed July 2018].
- [9]. H. Liu, H. Darabi, P. Banerjee, J. Liu, Survey of Wireless Indoor Positioning Techniques and Systems, *IEEE Transactions on Systems, Man, and Cybernetics*, Vol. 37, Issue 6, 2007, pp. 1067-1080.
- [10]. S. Tekinay, E. Chao, R. Richton, Performance benchmarking for wireless location systems, *IEEE Communications Magazine*, Vol. 36, Issue 4, 1998, pp. 72-76.
- [11]. E. Tinti, Metodi e Stumenti per il Posizionamento Indoor, Università di Bologna-Campus Di Cesena - Scuola Di Scienze, Bologna, Anno Accademico, 2014.
- [12]. S. Ingram, D. Harmer, M. Quinlan, Ultrawideband indoor position systems and their use in emergencies, in *Proceedings of the Position Location and Navigation Symposium*, Monterey, CA, USA, 2004.
- [13]. P. Pannuto, B. Kempke, L.-X. Chuo, D. Blaauw, P. Dutta, Harmonium: Ultra Wideband Pulse Generation with Bandstitched Recovery for Fast, Accurate, and Robust Indoor Localization, *ACM Transactions on Sensor Networks*, Vol. 14, Issue 2, 2018, p. Article 11.
- [14]. R. F. Brena, P. Garcia-Vazquez, C. E. Galván-Tejada, D. Muñoz-Rodríguez, C. Vargas-Rosales, J. Fangmeyer Jr., Evolution of Indoor Positioning Technologies: A Survey, *Journal of Sensors*, Vol. 2017, 2017, Article ID 2630413.
- [15]. A. Yassin, *et al.*, Recent Advances in Indoor Localization: A Survey on Theoretical Approaches and Applications, *IEEE Communications Surveys & Tutorials*, Vol. 19, Issue 2, 2017, pp. 1327-1246.
- [16]. G. Mao, B. Fidan, Localization Algorithms and Strategies for Wireless Sensor Networks, *Information science Reference-Imprint of IGI Publishing*, 2009.
- [17]. R. Kaune, J. Horst, W. Koch, Accuracy Analysis for TDOA Localization in Sensor Networks, in *Proceedings of the 14<sup>th</sup> International Conference on Information Fusion*, Chicago, Illinois, USA, 2011.
- [18]. U. Yayan, H. Yucel, A. Yazici, A Low Cost Ultrasonic Based Positioning System for the Indoor Navigation of Mobile Robots, *Journal of Intelligent & Robotic Systems*, Vol. 78, Issue 3-4, 2015, pp. 541-552.
- [19]. Y. Zhou, An efficient least-squares trilateration algorithm for mobile robot localization, in *Proceedings of the IEEE/RSJ International Conference on Intelligent Robots and Systems*, 2009, pp. 3474-3479.
- [20]. K. W. Cheung, H. C. So, W.-K. Ma, Y. T. Chan, A Constrained Least Squares Approach to Mobile Positioning, *EURASIP Journal on Applied Signal Processing*, 2006, pp. 1-23.
- [21]. S. J. Wright, J. Nocedal, Numerical Optimization, Springer, 1999.
- [22]. E. Electronics, Engineeringshock Electronics, 2018. [Online]. <http://www.engineeringshock.com/ultrasonics.html>. [Accessed 23 May 2019]
- [23]. R. M. Freund, The Steepest Descent Algorithm for Unconstrained Optimization and a Bisection Line-search Method, *Massachusetts Institute of Technology*, Massachusetts, 2004.
- [24]. A. J. Burns, S. Fichera, P. Paoletti, A low cost ultrasound-based localisation system, in *Proceedings of the 1<sup>st</sup> IFSA Frequency & Time Conference (IFTC'19)*, Tenerife (Canary Islands), 25-27 September 2019, pp. 21-27.



Published by International Frequency Sensor Association (IFSA) Publishing, S. L., 2019 (<http://www.sensorsportal.com>).



### Universal Frequency-to-Digital Converter (UFDC-1)

- 16 measuring modes: frequency, period, its difference and ratio, duty-cycle, duty-off factor, time interval, pulse width and space, phase shift, events counting, rotation speed
- 2 channels
- Programmable accuracy up to 0.001 %
- Wide frequency range: 0.05 Hz ... 7.5 MHz (120 MHz with prescaling)
- Non-redundant conversion time
- RS-232, SPI and I<sup>2</sup>C interfaces
- Operating temperature range -40 °C... +85 °C

[www.sensorsportal.com](http://www.sensorsportal.com)    [info@sensorsportal.com](mailto:info@sensorsportal.com)    SWP, Inc., Canada